ScienceDirect

Materials Science and Engineering: C

Volume 93, 1 December 2018, Pages 623-629

Short communication

Catalytic reduction of p-nitrophenol and methylene blue by microbiologically synthesized silver nanoparticles

Pranjali S. Rajegaonkar [a], Bhakti A. Deshpande [a], Manjushri S. More [a], Shivaji S. Waghmare [b], Vishal V. Sangawe [c], Areeb Inamdar [c], Mahendra D. Shirsat [d], Nitin N. Adhapure [c]

Show more

Outline | Share Cite

https://doi.org/10.1016/j.msec.2018.08.025

Get rights and content

Highlights

- Extracellular silver nanoparticles have excellent catalytic activity in reduction of p-nitrophenol.
- Immobilized intra and extracellular AgNPs have good methylene blue reduction ability.
- The XRD pattern confirms the face centered cubic (fcc) structure of nano silver.
- TEM images reveal the presence of multidispersive nanosilver with varying size 4.7 nm, 6.8 nm and 18.8 nm with mean particle size 10.1 nm and exhibiting roughly spherical morphology.

Abstract

Catalytic Reduction of p-nitrophenol and Methylene blue by Microbiologically Synthesized Silver

Nanoparticles was studied in the present investigation. Catalytic reduction of 4-Nitophenol/p-nitrophenol (PNP) and methylene blue (MB) was assessed using both intra and extracellular silver nanoparticles (AgNP) with and without immobilization. Both intracellular and extracellular AgNP were synthesized from actinomycetes. Antimicrobial activity of AgNP was also assessed and it was found that, intracellular AgNP have significant antibacterial activity against *E. coli*, *S. typhi and B. subtilis*. Synthesized biogenic silver nanoparticles were characterized by UV–visible spectrophotometry, FTIR, XRD, and TEM-EDS.

It was found that, extracellular AgNP are efficient as compared to intracellular AgNP in terms of PNP reduction.

Graphical abstract

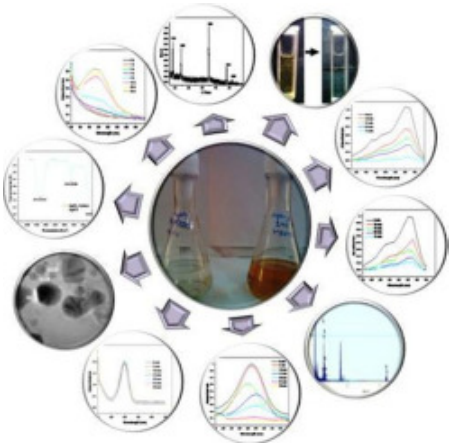

Download : Download high-res image (92KB)

Download : Download full-size image

Previous Next

1. Introduction

Nanoparticles from various metals, materials and their synthesis by physical, chemical and biological means are well reported in the literature [[1], [2], [3], [4]].

Green nanotechnology is gaining more attention due to its ecofriendly and economical approach to nanoparticles synthesis. Use of biological entities such as plants, plant extracts, bacteria, fungi, algae, diatoms, actinomycetes, and viruses have been emerging as a promising eco-friendly method for the synthesis of biogenic nanoparticles [5]. These nanoparticles are proved to be very effective in various fields [3,[6], [7], [8], [9]].

United States Environmental Protection Agency (US-EPA) has listed out 129 organic chemicals,

which are carcinogens and perilous to human beings as well as to the environment. Among these, 4-nitrophenol (4-NP) is one of the organic pollutants that are extensively used for the synthesis of drugs, dyes, insecticides and herbicides. Since it is readily soluble in water, 4-NP is abundantly present in the industrial effluents, soil and air. Further, it damages mitochondria and inhibits energy metabolism in human and animal. Nitrophenols are toxic and mutagenic organic pollutants used in the manufacturing of insecticides, fungicides, drugs and explosives [10]. So, the reduction or conversion of 4-NP to 4-aminophenol (4-AP) assumes greater importance both environmentally and industrially. Detoxification of organic pollutants remains as a stiff challenge to mankind and any significant contribution in this direction is of immense value worldwide [11]. It is readily degradable by various physical and chemical methodologies involving adsorption, photocatalysis, ozonation, UV irradiation, microwave, sonolysis, electrocatalysis, and Fenton reaction. Such methods are energy consuming and/or require organic solvents. An internally-irradiated annular photoreactor was used for the oxidative degradation of aqueous 4-NP with titania suspension as photocatalyst [12]. Heterogeneous Fenton-like reaction on nano-magnetite (Fe_3O_4) were demonstrated for the degradation of 4-nitrophenol (4-NP) [13].

Dyes are widely used in textile, paper, plastic, food and cosmetic industries. The wastes coming from these industries can affect on our atmosphere causing pollution. Many dyes are difficult to degrade. They are generally stable to light, oxidizing agents and are resistant to aerobic digestion [14]. Methylene blue is a thiazine dye used in many applications like aqua culture, anti-malarial drugs, chemotherapeutics and medicine [38]. It has a characteristic deep blue color in the oxidized state, but the reduced form, leukomethylene blue (LMB), is colorless. Methylene blue has been widely used in a variety of clinical settings to identify anatomic [15] and pathologic [[16], [17], [18]] structures and to treat met hemoglobinemia [[19], [20], [21]]. Some latest research articles have reported the decolourization of methylene blue by adsorption [[22], [23], [24], [25], [26], [27]].

In addition to adsorption, catalytic reduction of dyes has also emerged as effective way of decolorization. Metal nanoparticles have received great attention due to their catalytic role in the reduction and degradation of dyes. Among the noble metals, silver nanoparticles (AgNP) have become the focus of intensive research, because of low cost and emerging applications. Use of biogenic nanoparticles, being an environmentally benign greener option, is very much preferred in a variety of applications [11]. AgNP act as a redox catalyst in the degradation of dyes by electron relay effect between donor and acceptor molecules [28]. Reduction of Ag^+ ions and synthesized silver nanoparticles having chemo-catalytic potential in reduction of 4-nitrophenol (4-NP) to 4- amino phenol (4-AP), was demonstrated by Seralathan et al., [29].

To the best of our knowledge, this is the first report for “Utilization of AgNps from Actinomycetes for detoxifying the hazardous pollutants 4NP and Methylene blue”. There are few recent reports highlighting on catalytic reduction of 4NP, however, none of these reports have utilized nanoparticles synthesized from Actinomycetes. Actinomycetes being filamentous bacteria are a better source for biological synthesis of nanoparticles.

Moreover, both the intra and extra cellular nanoparticles have been tested for catalytically reducing 4NP and MB, such comparison is not previously reported and hence worth knowing.

In present study we have synthesized both intra and extra cellular silver nanoparticles from a filamentous bacteria actinomycetes and these synthesized AgNP were used for catalytically reducing 4-NP and Methylene blue. In addition to that, immobilized AgNP were also used for catalytic activity assessment.

2. Materials and methods

2.1. Isolation and identification of actinomycetes

For isolation of actinomycetes five different soil samples were collected from various sites of Jalna city (M.S.) India. Soil, three inches below from surface was collected in polythene bags and brought to the laboratory for further studies.

The actinomycetes were isolated by serial dilution technique using 0.1 mL of 10^{-7} dilution [39] on Bennet's agar supplemented with antifungal antibiotic griseofulvin at 50 μg/mL concentration [40]. Actinomycetal growth was observed by incubating the Plates at room temperature for 5–6 days.

The isolated colonies were preserved on Bennet's agar slants supplemented with antifungal grisofilvin for further studies. Among the obtained 10 isolates isolate IN-8 and MRS- 1 were selected for intracellular and extracellular AgNP synthesis.

2.2. Synthesis of intracellular AgNP

The MGYP medium was inoculated with loop full culture of isolated actinomycetes and incubated in rotary shaker incubator at 120 rpm, 30 °C for 2–3 days.

Biomass was collected and washed with double distilled water for two to three times. After this, the biomass was transferred to the silver nitrate solution (10^{-3} M) and incubated for 12 days in shaking incubator.

2.3. Synthesis of extracellular AgNP

The MGYP medium was inoculated with loop full culture of isolated actinomycetes and incubated in shaking incubator at 120 rpm, 30 °C for 2–3 days.

After incubation biomass was removed and 5 ml of MGYP broth was transferred to the silver nitrate solution (10^{-3} M) and the flask was incubated for 2–3 days in shaking incubator adjusted at 120 rpm, 30 °C.

2.4. Characterization of synthesized AgNP

The formation of AgNP was monitored by visible color change, UV–Visible Spectrophotometer

(ELICO-BL222) at an interval of 50 nm between 190 and 700 nm and FTIR spectral analysis to analyze possible functional group present. Bruker (EcoATR) ALPHA, was employed to collect IR spectra of liquid phase extracellular AgNP, examined in the diffuse transmittance mode operating at a resolution of 4 cm^{-1} over 4500–500 cm^{-1}.

The nanostructure of silver was characterized by using X-ray diffraction using Brucker D 8 advanced diffractometer.

The TEM studies were carried out for better examination of size, morphology and dispersity of the synthesized nanoparticles. Elemental analysis of sample was done by robust technique of Energy dispersive X-ray spectroscopy. The size and morphology of silver nanoparticles were determined by TEM, Tecnai T20 Edax RTEM SN9577 microscope, operating at 200 kv equipped with an EDS detector.

2.5. Catalytic reduction of 4-NP and MB by AgNP's

The catalytic potential of both extracellular and intracellular AgNP was assessed by reducing 4-NP and MB and was monitored by UV–visible spectrophotometer.

2.5.1. Catalytic reduction of 4-NP by extracellular and intracellular AgNP

The AgNP were used for catalytically reducing 4-NP in presence of $NaBH_4$ which act as potential reducing agent. The catalytic activity of extracellular and intracellular AgNP was assessed in three different reaction mixtures prepared for both type of nanoparticles i.e. intracellular and extracellular separately. In first reaction mixture, 0.5 ml of 4-nitrophenol (0.5 mM) was added with 1.5 ml of distilled water. In second reaction mixture, 0.5 ml of 4-nitrophenol, 1.5 ml of distilled water and 1 ml of $NaBH_4$ (0.02 M) was added and in third reaction mixture, 0.5 ml of 4-nitrophenol, 1.5 ml of distilled water, 1 ml of $NaBH_4$ and 15 μl of AgNP were added. The absorbance of all three reaction mixtures was monitored by UV–visible spectrophotometer from 0 to 30 min with successive time interval of 5 min.

2.5.2. Catalytic reduction of MB by extracellular and intracellular AgNP

Catalytic reduction of MB (5 ppm) by extracellular and intracellular AgNP was assessed. The test sample was prepared by adding 0.2 mL AgNP to 1 mL of MB and 1.8 mL of distilled water (now final concentration of AgNP would be 11.3 μg/mL). The control mixture contains 1 mL of MB added with 2 mL of distilled water. The absorbance was monitored on UV–visible spectrophotometer with successive interval of 15 min starting from 30 min of incubation to 75 min.

2.6. Immobilization of AgNP

Immobilization of AgNP was carried out by using 4% Sodium alginate and 1 M chilled $CaCl_2$ solution. The sodium alginate beads were formed by mixing equal proportion of AgNP and sodium alginate solution, followed by suspending mixture in $CaCl_2$ solution. The control sodium alginate beads were

formed by mixing sodium alginate with equal quantity of distilled water instead of AgNP. The formed beads were placed in $CaCl_2$ solution for cross-linking, to achieve additional stability. After 24 h of cross-linking, the beads were filtered and washed 3–4 times with NaCl and were used for further experiments.

2.7. Catalytic reduction of MB by immobilized intracellular and extracellular AgNP

The catalytic activity of immobilized extracellular and intracellular AgNP was analyzed separately by performing the following experiments. In a test tube, 10 mL MB (5 PPM) and 100 control beads were taken, while in a second test tube, 10 mL MB (5 PPM) and 100 intracellular immobilized AgNP beads were taken. Reduction of methylene blue by AgNP was monitored in terms of change in absorbance over the period of time. The absorbance was monitored on UV–visible spectrophotometer after 30, 45, 60 and 75 min of incubation.

2.8. Antimicrobial activity of AgNP

The antimicrobial activity of silver nanoparticles was tested by disc diffusion method against five phytopathogenic fungus viz. *Alternaria*, *Curvularia*, *Fusarium*, *A. flavus*, *A. niger* and four bacterial culture viz. *S. aureus*, *B. subtilis*, *S. typhi* and *E. coli*.

The Potato Dextrose agar plates were inoculated with selected fungal and nutrient agar plates were inoculated with selected bacterial cultures. Sterile paper discs were soaked in AgNP solutions. The disks were prepared as Disc-A = extracellular nanoparticles, Disc-B = $AgNO_3$ solution, Disc-C = Dust of intracellular nanoparticles, Disc-D = Biomass of extracellular nanoparticles and Disc-E = Biomass of intracellular nanoparticles. The soaked discs were placed in potato dextrose agar plates and nutrient agar plates separately. The plates were then incubated at room temperature for 24–48 h. Standard Antibacterial (Penicillin and Ampicillin) and antifungal agents (Fluconazole) were used as positive controls.

3. Results and discussion

3.1. Biosynthesis of AgNP

Biomass in the form of beads was obtained after five days of incubation in rotary shaking incubator at 30 °C. The obtained biomass was then used for further studies. Spectrophotometric studies reveal that, silver nanoparticles were synthesized from actinomycetes in aqueous $AgNO_3$ solution. A visible color change (Fig. 1) and increase in absorbance (Fig. 2) from colorless to brown after incubation is signature sign of synthesized nanoparticles [41].

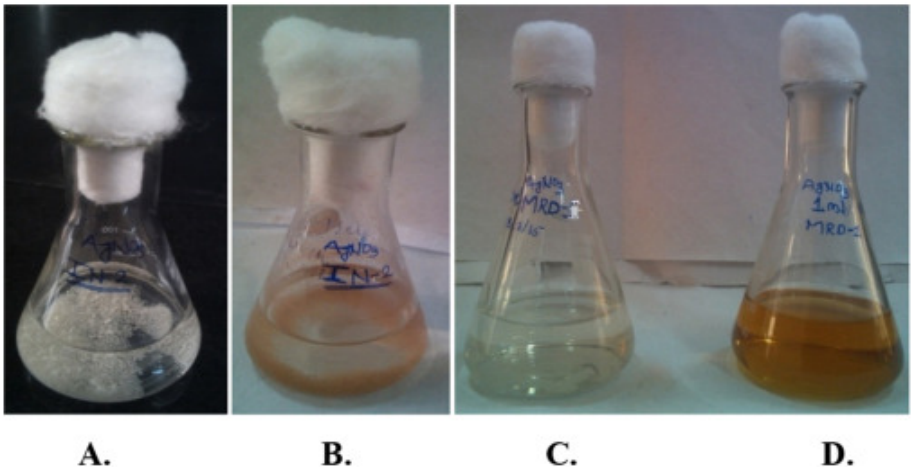

Download : Download high-res image (153KB)

Download : Download full-size image

Fig. 1. Biosynthesis of AgNP, Intracellular A. At 0 h B. After 7 days, Extracellular, C. 0 min D. 24 h.

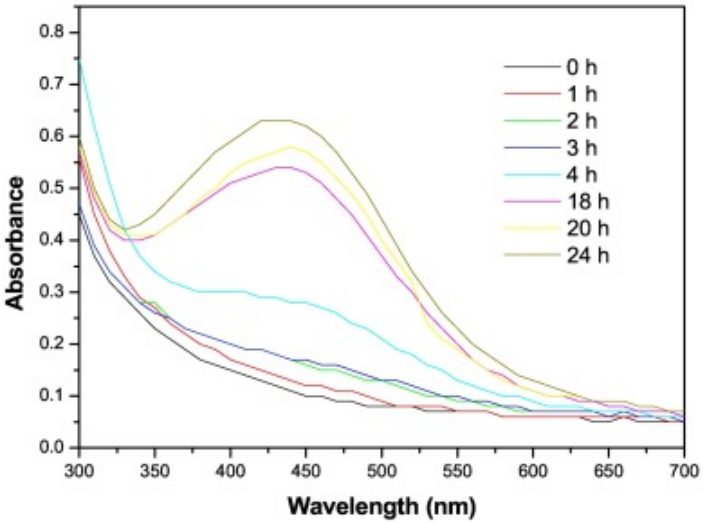

Download : Download high-res image (204KB)

Download : Download full-size image

Fig. 2. Biosynthesis of extracellular AgNP.

3.2. Characterization of AgNP

Synthesized silver nanoparticles in aqueous $AgNO_3$ solution was examined by using UV–visible spectrophotometer and FTIR spectral analysis. The experimental samples was observed with change in color from colorless to yellowish-brown with surface plasmon resonance (SPR) band centered at 435 nm after 24 h. The characterization was carried out by XRD for determining structure and crystallinity. The TEM studies were carried out for better examination of size, morphology and dispersity of the synthesized nanoparticles. Elemental analysis of sample was done by robust

technique of Energy dispersive X-ray spectroscopy.

3.2.1. Fourier Transform Infrared (FTIR) analysis

FTIR spectra (Fig. 3) shows absorption peak located at about 3335.28, 2109.74, 1636.3 and 785.85 cm^{-1}. The band at 1636.3 is due to C═O stretching vibrations present in the amide linkages of the proteins. The peak at 3335.28 cm^{-1} is associated with N—H stretching vibration present in the amide linkages of the proteins, such peak is also associated with O—H stretching vibrations. Weak peak at 785.85 indicates C—H bend.

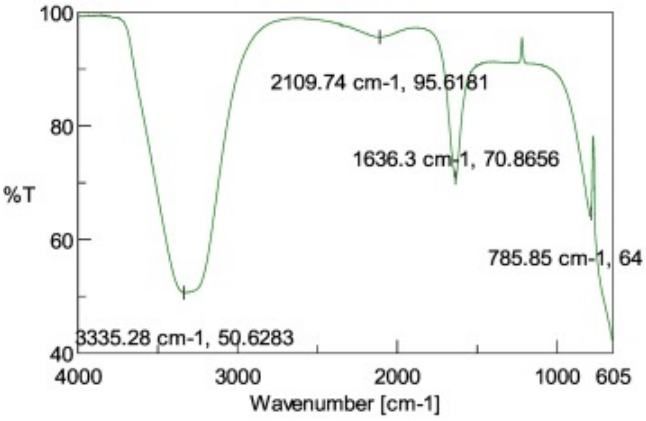

Download : Download high-res image (137KB)

Download : Download full-size image

Fig. 3. FTIR Spectra of silver nanoparticles synthesized by microbes [Brucker (EcoATR) ALPHA].

The peaks obtained may suggest that, the biological molecules possibly perform dual function of synthesis and stabilization of silver nanoparticles (R. [30]). It is well known fact that, proteins can bind to silver nanoparticles through free amine groups and thereby stabilize the silver nanoparticles.

3.2.2. X-ray diffraction analysis

The XRD profile (Fig. 4) of silver nano particles exhibits characteristic peaks at scattering angles (2Θ) of 38.23°, 44.41°, 64.65°, 77.65° and 81.59° corresponding to scattering hkl values 111, 200, 220, 311 and 222 respectively. The obtained peaks are consistent with the face centered cubic (fcc) structure of silver, and can be assigned to JCPDS File No. 04-0783. [31].

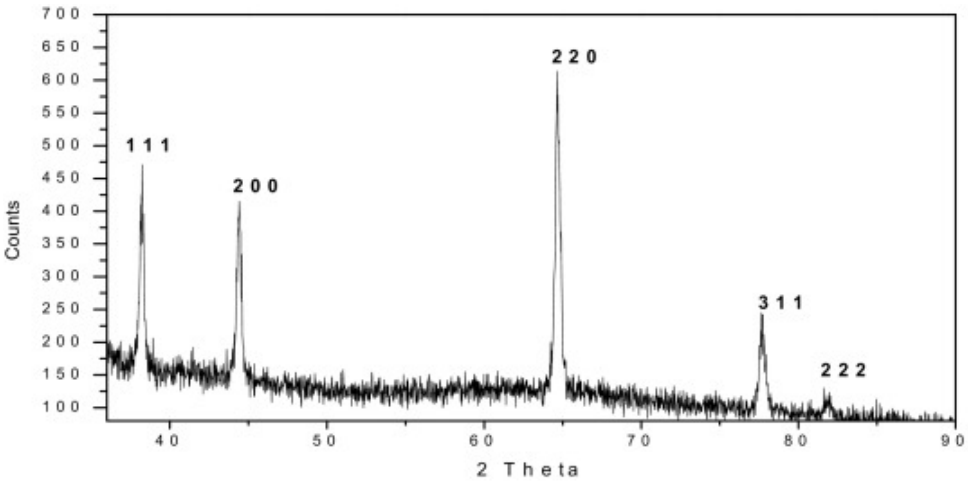

Download : Download high-res image (182KB)

Download : Download full-size image

Fig. 4. X-ray diffraction pattern of crystalline silver nanoparticles.

The intensities of the diffraction pattern were observed as peak heights and are mentioned in Table 1. According to Alexander et al. [32], the intensity patterns can be helpful for commenting on average particle size. Considering this, the well defined intense peaks (Fig. 4 and Table 1) confirm excellent crystallinity as well as nano sized silver particles.

Table 1. Comparison of Inter-planer spacings (d_{hkl}) from standard silver diffraction data (JCPDS file no. 04-0783) with the experimentally observed values from XRD diffractogram.

JCPDS NO: 04-0783			**Observations of XRD**		
d_{hkl} (A^0)	**Intensity**	**hkl values**	**2Θ**	**Intensity**	**Observed d_{hkl} (A^0)**
2.359	100	111	38.23	471	2.3619
2.044	40	200[a]	44.41	415	2.0455
1.445	25	220	64.65	614	1.434
1.231	26	311	77.65	245	1.2335
1.1796	12	222	81.59	130	1.1810

a Marlene et al. [33].

3.2.3. Surface morphology (TEM) and elemental (EDS) analysis

The sample was deposited on grid and air dried. The TEM grid for extracellular and intracellular

AgNP's were prepared before analysis and examined from different locations of the grid with different magnification. Examined particles were measured for size distribution using image software.

The extracellularly synthesized nanoparticles were found to be roughly spherical and with varying size 4.7 nm, 6.8 nm and 18.8 nm, the mean particles size was 10.1 nm (Fig. 5A). Investigation of intracellularly synthesized nanoparticle reveals their presence within mycelium with roughly spherical shape (Fig. 5B). The particles observed in TEM imaging was identified and confirmed as silver nanoparticles through EDS profile. Additional comparison of intracellular and extracellular elemental analysis reveals the presence of strong signals for carbon and AgNP in extracellular sample. However, in intracellular sample, strong signals for carbon and AgNP, and weak signals for oxygen, Nitrogen and sulphur were observed (Fig. 5C, D).

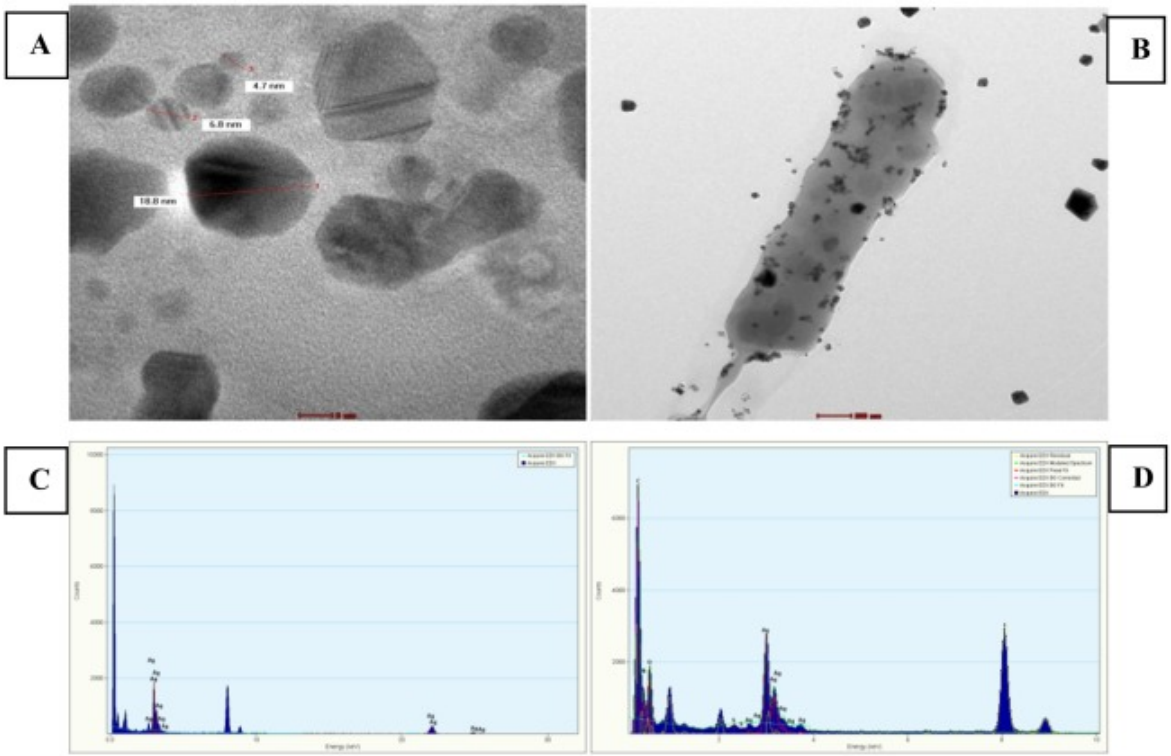

Download : Download high-res image (513KB)

Download : Download full-size image

Fig. 5. TEM and EDS profile.

A- TEM of extracellular AgNP, B- TEM of intracellular AgNP, C-EDS profile of extracellular AgNP, and D-EDS profile of intracellular AgNP [Energy (keV) Vs counts].

3.3. Catalytic reduction of 4-NP by extracellular and intracellular AgNP

The visual inspection and spectral pattern studies indicate reduction potential of biogenic AgNP which varies with incubation time.

The spectral line at 0 min (black band) and 5 min (red band) shows absorption maxima at 390 nm with no any conversion of 4-NP to 4-AP. Increase in incubation time results in shifting of band at 390 nm, and further incubation results in decrease in absorption with respect to shifting in bands exhibiting surface plasmon resonance (SPR) phenomenon. During the course of incubation, due to reduction of 4-NP to 4-AP by AgNP and transfer of electrons from BH_4^- ions to nitro compound, the yellow color of reaction mixture starts to fade, which was qualitatively measured. The reaction leads to formation of 4-AP (4-aminophenol) a colorless compound (Fig. 6, Fig. 7). Rapid reduction of 4-NP was observed with addition of minute quantity (15 μl) of biogenic AgNP which was also evident by various researchers viz., [[34], [35], [36]].

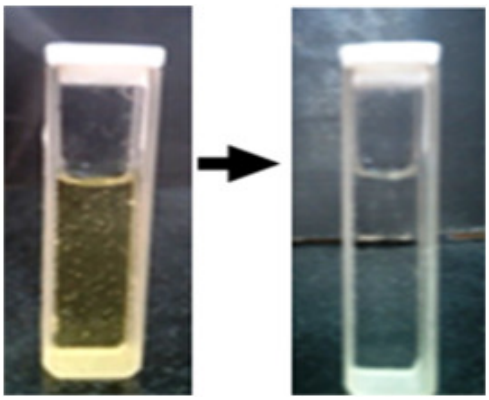

Download : Download high-res image (57KB)

Download : Download full-size image

Fig. 6. 4-nitrophenol reduction by extracellular AgNP after 30 min.

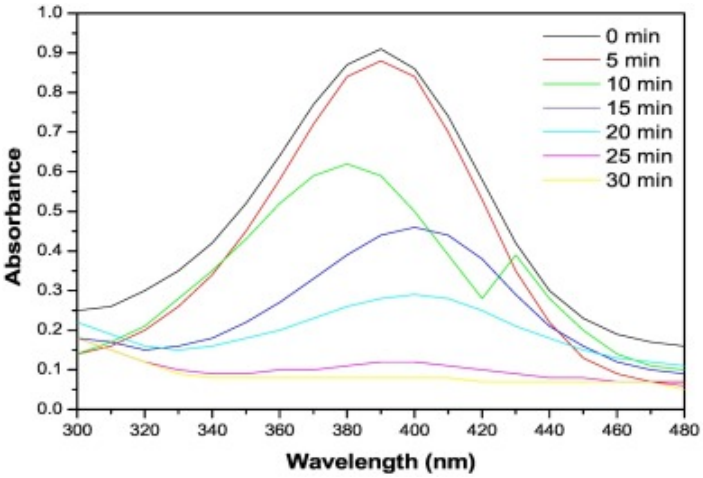

Download : Download high-res image (215KB)

Download : Download full-size image

Fig. 7. 4-nitrophenol reduction by extracellular AgNP.

Intracellular AgNP do not exhibit any catalytic activity of 4-NP reduction. This is evident by spectrophotometric analysis, as initially absorbance was 1.77 and after 30 min it remains same (Fig. 8). Visual inspection also indicates no change in color of reaction mixture.

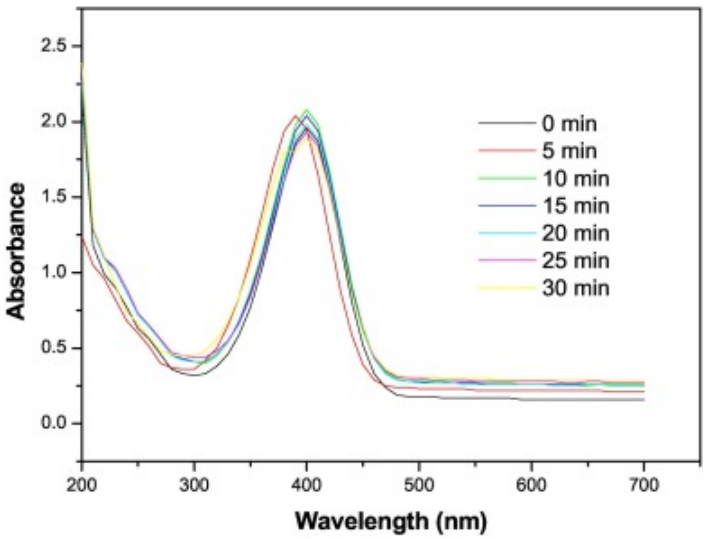

Download : Download high-res image (178KB)

Download : Download full-size image

Fig. 8. 4-nitrophenol degradation by intracellular AgNP.

Similar experiments of catalytic reduction of 4-NP were performed by using immobilized intracellular and extracellular AgNP but no catalytic reduction was observed.

3.4. Catalytic reduction of methylene blue by intracellular AgNP

The catalytic activity of AgNP for the methylene blue reduction was monitored by UV–visible spectrophotometer and the reduction was also confirmed by visual inspection. Pure MB has λ max value of 664 nm. After 30 min of incubation the spectrophotometric monitoring of test sample reveals decrease in absorbance (Fig. 9) as compared to control. Reaction mixture consisting of MB and intracellular AgNP was found to exhibit noticeable decrease in the absorbance of MB over the period of incubation.

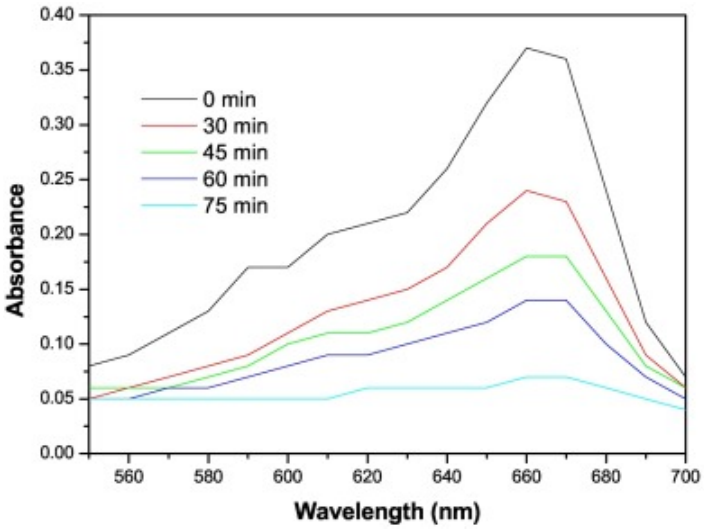

Download : Download high-res image (186KB)

Download : Download full-size image

Fig. 9. Methylene blue reduction by intracellular AgNP.

3.5. Catalytic reduction of MB by immobilized extracellular AgNP

The reduction of MB via immobilized AgNP spectral analysis annotated in spectra mentioned in Fig. 10. Decreased absorbance of MB in test sample over the time of incubation indicates catalytic reduction.

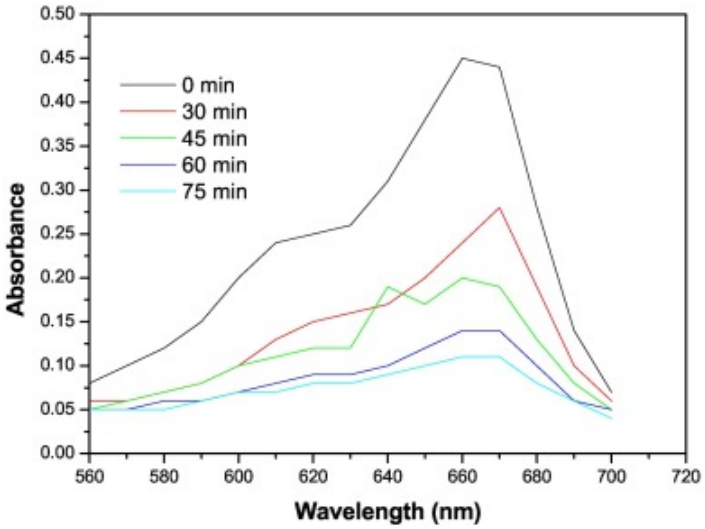

Download : Download high-res image (185KB)

Download : Download full-size image

Fig. 10. Methylene blue reduction by immobilized beads of extracellular AgNP.

The MB reduction by silver nanoparticles is governed by electron relay system, where the catalytic

reduction of MB is based on electron transfer between MB and Ag^+, here MB acts as redox catalyst during reaction, the phenomenon is known as electron relay system [37].

3.6. Antimicrobial activity of AgNP

The antibacterial nature of extracellular AgNP against *S. typhi*, *E. coli*, *S. aureus and B. subtilis* was studied. While comparing with the standard antibiotics, it was found that, the extracellular AgNP have potent activity against *S. typhi* and *B. subtilis* with zone of inhibition 8 mm and 10 mm respectively. Intracellular AgNP also showed good antimicrobial activity against *S. typhi* (7 mm) and *B. subtilis* (8 mm).

However both intra and extracellular silver nanoparticles do not have potential antifungal activity against the tested fungal cultures.

4. Conclusions

Actinomycetes were found effective producer of AgNP, while considering the greener approach for synthesis of nanoparticles. To the best of our knowledge this is first report of its kind for utilization of AgNP previously synthesized from actinomycetes, and their application for reducing 4-Nitrophenol and methylene blue. Extracellular AgNP found to have excellent catalytic activity in terms of 4-NP and MB reduction. In addition, both immobilized intracellular and extracellular AgNP proved to have good methylene blue reduction ability. The XRD and TEM analysis confirms FCC structure of nanosilver and presence of multidispersive nanoparticles with mean size 10.1 nm, respectively.

References

[1] Shu-Hua Liu, Haita G. Enyi Ye, Michelle Low, Hon Lim Su, Shuang-Yuan Zhang, Xiaohui Lieu, Sudhiranjan Tripathy, Wolfgang Tremel, Ming-Yong Han, *et al.*
Graphitically encapsulated cobalt nanocrystal assemblies
Chem. Commun., 46 (2010), pp. 4749-4751
CrossRef ↗ View in Scopus ↗ Google Scholar ↗

[2] Enyi Ye, Shuang-Yuan Zhang, Suo Hon Lim, Shuhua Liu, Ming-Yong Han
Morphological tuning, self-assembly and optical properties of indium oxide nanocrystals
Phys. Chem. Chem. Phys., 12 (2010), pp. 11923-11929
CrossRef ↗ View in Scopus ↗ Google Scholar ↗

[3] Enyi Ye, Shuang-Yuan Zhang, Suo Hon Lim, Michel Bosman, Zhihua Zhang, Khin Yin Win, Ming-Yong

Han
Ternary cobalt–iron phosphide nanocrystals with controlled compositions, properties, and morphologies from nanorods and nanorice to split nanostructures
Chem. Eur. J., 17 (2011), pp. 5982-5988
CrossRef ↗ View in Scopus ↗ Google Scholar ↗

[4] N.L. Gavade, A.N. Kadam, M.B. Suwarnkar, V.P. Ghodake, K.M. Garadkar, A. Malhotra, K. Dolma, N. Kaur, Y.S. Rathore, S. Ashish Mayilraj, A.R. Choudhury
Biosynthesis of gold and silver nanoparticles using a novel marine strain of Stenotrophomonas
Bioresour. Technol., 142 (2013), pp. 727-731
Google Scholar ↗

[5] K.B. Narayanan, H.H. Park, N. Sakthivel
Extracellular synthesis of mycogenic silver nanoparticles by *Cylindro caladium floridanum* and its homogeneous catalytic degradation of 4-nitrophenol
Spectrochim. Acta A Mol. Biomol. Spectrosc., 116 (2013), pp. 485-490
View PDF View article View in Scopus ↗ Google Scholar ↗

[6] Enyi Ye, Hua Tan, Shuping Li, Wai Yip Fan
Self-organization of spherical, core–shell palladium aggregates by laser-induced and thermal decomposition of [Pd(PPh3)4]
Angew. Chem. Int. Ed., 45 (2006), pp. 1120-1123
CrossRef ↗ View in Scopus ↗ Google Scholar ↗

[7] Qing Qing Dou, Hong Chen Guo, Enyi Ye
Near-infrared upconversion nanoparticles for bio-applications
Mater. Sci. Eng. C, 45 (2014), pp. 635-643
View PDF View article View in Scopus ↗ Google Scholar ↗

[8] Shuang-Yuan Zhang, Enyi Ye, Shuhua Liu, Suo Hon Lim, Si Yin Tee, Zhili Dong, Ming-Yong Han
Temperature and chemical bonding-directed self-assembly of cobalt phosphide nanowires in reaction solutions into vertical and horizontal alignments
Adv. Mater., 24 (2012), pp. 4369-4375
CrossRef ↗ View in Scopus ↗ Google Scholar ↗

[9] Vahid Hosseini, Silvan Gantenbein, Ima Avalos Vizcarra, Ingmar Schoen, Viola Vogel
Stretchable silver nanowire microelectrodes for combined mechanical and electrical stimulation of cells
Adv. Healthc. Mater., 1–10 (2016), 10.1002/adhm.201600045 ↗
Google Scholar ↗

[10] W.B. Zhang, X. Xiao, T. An, Z. Song, J. Fu, G. Sheng, M. Cui, J. Chem
Kinetics degradation pathway and reaction mechanism of advanced oxidation of 4-nitrophenol in water by H_2O_2 process
J. Chem. Technol. Biotechnol., 78 (2003), pp. 788-794
View in Scopus ↗ Google Scholar ↗

[11] Jebakumar T. Immanuel Edison, M.G. Sethuraman
Biogenic robust synthesis of silver nanoparticles using Punica granatum peel and its application as a green catalyst for the reduction of ananthropogenic pollutant4-nitrophenol
Spectrochim. Acta A Mol. Biomol. Spectrosc., 104 (2013), pp. 262-264
View in Scopus ↗ Google Scholar ↗

[12] J. Lea, A.A. Adesina, J. Chem
Oxidative degradation of 4 nitrophenol in UV illuminated titania
J. Chem. Technol. Biotechnol., 76 (2001), pp. 803-810
Google Scholar ↗

[13] S.P. Sun, A.T. Lemley
p-Nitrophenol degradation by a heterogeneous Fenton-like reaction on nano-magnetite: process optimization, kinetics, and degradation pathways
J. Mol. Catal. A Chem., 349 (2011), pp. 71-79
View PDF View article View in Scopus ↗ Google Scholar ↗

[14] G. McKay, A. Sweeney
Principles of dye removal from textile effluent
Water Air Soil Pollut., 14 (1980), pp. 3-11
Google Scholar ↗

[15] H. Manhes, A. Shulman, T. Haag, M. Canis, Demontmarin
Infertility due to diseased pelvic peritoneum: laparoscopic treatment
Gynecol. Obstet. Investig., 37 (1994), pp. 191-195
CrossRef ↗ View in Scopus ↗ Google Scholar ↗

[16] M.I.F. Canto, S. Setrakian, R.E. Petras, E. Blades, A. Chak, M.V. Sivak
Methylene blue selectively stains intestinal metaplasia in Barrett's esophagus
Gastrointest. Endosc., 44 (1996), pp. 1-7
View PDF View article View in Scopus ↗ Google Scholar ↗

[17] A.F. Derom, P.C. Wallaert, H.M. Janzing, E. Derom
Intra operative identification of para thyroid glands with Methylene blue infusion

Am. J. Surg., 165 (1993), pp. 380-382

View PDF View article View in Scopus ↗ Google Scholar ↗

[18] M. Lee, R. Sharifi
Methylene blue versus indigo carmine [letter]
Urology, 47 (1996), pp. 783-784

View PDF View article View in Scopus ↗ Google Scholar ↗

[19] S. Curry
Methemoglobinemia
Ann. Emerg. Med., 11 (1982), pp. 214-221

View PDF View article View in Scopus ↗ Google Scholar ↗

[20] F.D. Ellis, J.G. Seiler III, M.M. Palmore
Met hemoglobinemia: a complication after fiber optic or otracheal intubation with benzocaine spray
J. Bone Joint Surg. Am., 77 (1995), pp. 937-939

CrossRef ↗ View in Scopus ↗ Google Scholar ↗

[21] C.C. Yang, S.F. Hwang, M.M. Chou, J.F. Deng
Metobrumuron/metachlorine gestion with late onset methemoglobinemia in a pregnant woman successfully treated with methylene blue
J. Toxicol. Clin. Toxicol., 33 (1995), pp. 713-716

CrossRef ↗ View in Scopus ↗ Google Scholar ↗

[22] Ali Akbar Bazrafshan, Mehrorang Ghaedi, Shaaker Hajati, Reza Naghiha, Arash Asfaram
Synthesis of ZnO-nanorod-based materials for antibacterial, antifungal activities, DNA cleavage and efficient ultrasound-assisted dyes adsorption
Ecotoxicol. Environ. Saf., 142 (2017), pp. 330-337

View PDF View article View in Scopus ↗ Google Scholar ↗

[23] Arash Asfaram, Mehrorang Ghaedi, Kheibar Dashtian, Gholam Reza Ghezelbash
Preparation and characterization of $Mn_{0.4}Zn_{0.6}Fe_2O_4$ nanoparticles supported on dead cells of *Yarrowia lipolytica* as a novel and efficient adsorbent/biosorbent composite for the removal of azo food dyes: central composite design optimization study
ACS Sustain. Chem. Eng., 6 (4) (2018), pp. 4549-4563

CrossRef ↗ View in Scopus ↗ Google Scholar ↗

[24] Arash Asfaram, Mehrorang Ghaedi, Mohammad Hossein Ahmadi Azqhandi, Alireza Goudarzi, Shaaker Hajati

Ultrasound-assisted binary adsorption of dyes onto Mn@ CuS/ZnS-NC-AC as a novel adsorbent: application of chemometrics for optimization and modeling
J. Ind. Eng. Chem., 54 (2017), pp. 377-388
View PDF View article View in Scopus Google Scholar

[25] Ebrahim Alipanahpour Dil, Mehrorang Ghaedi, Arash Asfaram
The performance of nanorods material as adsorbent for removal of azo dyes and heavy metal ions: application of ultrasound wave, optimization and modeling
Ultrason. Sonochem., 34 (2017), pp. 792-802
View PDF View article View in Scopus Google Scholar

[26] H. Mazaheri, M. Ghaedi, M.H. Ahmadi Azqhandi, A. Asfaram
Application of machine/statistical learning, artificial intelligence and statistical experimental design for the modeling and optimization of methylene blue and Cd(II) removal from a binary aqueous solution by natural walnut carbon
Phys. Chem. Chem. Phys., 19 (2017), pp. 11299-11317
View in Scopus Google Scholar

[27] Mohammad Safarpoor, Mehrorang Ghaedi, Arash Asfaram, Masoumeh Yousefi-Nejad, Hamedreza Javadian, Hossein Zare Khafri, Marzieh Bagherinasab
Ultrasound-assisted extraction of antimicrobial compounds from *Thymus daenensis* and *Silybum marianum*: antimicrobial activity with and without the presence of natural silver nanoparticles
Ultrason. Sonochem., 42 (2018), pp. 76-83
View PDF View article View in Scopus Google Scholar

[28] K. Mallick, M. Witcomb, M. Scurrell
Silver nanoparticles catalysed redox reaction: an electron relay effect
Mater. Chem. Phys., 97 (2006), pp. 283-287
View PDF View article View in Scopus Google Scholar

[29] J. Seralathana, P. Stevensona, S. Subramaniama, R. Raghavana, B. Pemaiahb, A. Sivasubramaniana, A. Veerappan
Spectroscopy investigation on chemo-catalytic, free radical scavenging and bactericidal properties of biogenic silver nanoparticles synthesized using *Salicornia brachiata* aqueous extract
Spectrochim. Acta A Mol. Biomol. Spectrosc., 118 (2014), pp. 349-355
Google Scholar

[30] R. Sathyavathi, M. Balamurali Krishna, S. Venugopal Rao, R. Saritha, D. Narayana Rao
Biosynthesis of silver nanoparticles using *Coriandrum sativum* leaf extract and their

application in nonlinear optics

Adv. Sci. Lett., 3 (2010), pp. 138-143

CrossRef ↗ View in Scopus ↗ Google Scholar ↗

[31] Nityananda Agasti, N.K. Kaushik

One pot synthesis of crystalline silver nanoparticles

Am. J. Nanomater., 2 (2014), pp. 4-7

Google Scholar ↗

[32] L. Alexander, H. Klug

Basic aspects of X ray absorption in quantitative diffraction analysis of powder mixtures

Anal. Chem., 20 (10) (1948), pp. 886-889

CrossRef ↗ View in Scopus ↗ Google Scholar ↗

[33] Marlene C. Morris, Howard F. McMurdie, Eloise H. Evans, Boris Paretzkin, Harry S. Parker, Nicolas C. Panagiotopoulos

X-ray Diffraction Powder Pattern, BS Monograph 25 Section 18

U S Department of Commerce, National Bureau of standards (1981)

Google Scholar ↗

[34] S.A. Aromal, D. Philip

Green synthesis of gold nanoparticles using *Trigonella foenum-graecum* and its size-dependent catalytic activity

Spectrochim. Acta A Mol. Biomol. Spectrosc., 97 (2012), pp. 1-5

Google Scholar ↗

[35] N. Pradhan, A. Pal, T. Pal

Silver nanoparticle catalyzed reduction of aromatic nitro compounds

Colloids Surf. A Physicochem. Eng. Asp., 196 (2002), pp. 247-257

View PDF View article View in Scopus ↗ Google Scholar ↗

[36] H. Zhang, X. Li, G. Chen

Ionic liquid-facilitated synthesis and catalytic activity of highly dispersed Ag nanoclusters supported on TiO_2

J. Mater. Chem., 19 (2009), pp. 8223-8231

CrossRef ↗ View in Scopus ↗ Google Scholar ↗

[37] Jebakumar T. Immanuel Edison, M.G. Sethuraman

Instant green synthesis of silver nanoparticles using Terminaliachebul a fruit extract and evaluation of their catalytic activity on reduction of Methylene blue

Process Biochem., 47 (2012), pp. 1351-1357

View in Scopus Google Scholar

[38] V.K. Vidhu, Daizy Philip
Spectroscopic, microscopic and catalytic properties of silver nanoparticles synthesized using Saraca indica flower
Spectrochim. Acta A Mol. Biomol. Spectrosc., 1386-1425, 117 (2014), pp. 102-108
View PDF View article View in Scopus Google Scholar

[39] C.H. Collins, Patricia M. Lyne, J.M. Grange, J.O. Falkinham III
Recent Res. Sci. Technol.
Butterworth-Heinemann Publisher (1995), pp. 129-131
CrossRef View in Scopus Google Scholar

[40] R.M. Gulve, A.M. Deshmukh
Enzymatic activity of actinomycetes isolated from aarine aediments
Recent Research in Science and Technology, 3 (5) (2011), pp. 80-83
Google Scholar

[41] A. Malhotra, K. Dolma, N. Kaur, Y.S. Rathore, Ashish
Biosynthesis of gold and silver nanoparticles using a novel marine strain of Stenotrophomonas
Bioresour. Technol., 142 (2013), pp. 727-731
View PDF View article View in Scopus Google Scholar

Cited by (22)

Rhizospheric health management through nanofertilizers

2022, Rhizosphere Engineering

Show abstract

Hierarchical ZIF-decorated nanoflower-covered 3-dimensional foam for enhanced catalytic reduction of nitrogen-containing contaminants

2021, Journal of Colloid and Interface Science

> *Citation Excerpt :*
>
> …These results ascertained that ZIF@CF can be applied for reducing different analogues of nitrophenols. In addition to nitrophenols, many dye molecules are also NCCs and could be decolorized through reductive reactions by hydrogenating its nitrogen group of phenothiazine [46–48]. Thus, ZIF@CF was then also tested for

> these nitro-aromatic dyes, including MB and MO.…

Show abstract

One-step synthesized 3D-structured MOF foam for efficient and convenient catalytic reduction of nitrogen-containing aromatic compounds

2021, Journal of Water Process Engineering

> *Citation Excerpt :*
>
> …In addition to 4-NP reduction, the catalytic hydrogenation would be also employed for decolorizing dye-containing wastewater [66–68]. Specifically, Methylene blue (MB) represents an extensively-used dye and it could be decolorized by hydrogenate its nitrogen group of phenothiazine in MB [66–68]. Firstly, Fig. S4 shows a MB aqueous solution (curve a) and a MB solution in the presence of HKUST-1 foam after 300 min (curve b), indicating that adsorption of MB adsorbed to HKUST-1 was negligible.…

Show abstract

Ag(0) nanocatalyst stabilized with networks of p(SPA-co-AMPS) for the hydrogen generation process from ethylenediamine bisborane hydrolysis

2020, International Journal of Hydrogen Energy

> *Citation Excerpt :*
>
> …Silver nanoparticles (AgNPs) have unrivalled optical, biomedical, catalytic and sensor properties and have begun to be frequently used in the field of heterogeneous catalysis due to their low costs [31–35]. AgNPs may be obtained by biologic, physical and chemical methods [36]. With the chemical method, nanoparticules can be synthesized with reduction of Ag(I) ions using organic and inorganic reducing agents [37].…

Show abstract

AgNPs embedded N- doped highly porous carbon derived from chitosan based hydrogel as catalysts for the reduction of 4-nitrophenol

2019, Composites Part B: Engineering

> *Citation Excerpt :*
>
> …The silver nanoparticles (AgNPs) own not only high selectivity and quickly electron transportation abilities, but also have good recyclability due to their unique properties [11,12]. These features enable them acquiring high catalytic performance towards catalytic reduction of 4-NPs [13–16]. However, AgNPs suffer from serious stability problems such as aggregation in practice due to their high surface energy, eventually losing of their intrinsic activity [17].…

Show abstract

Bioinspired silver nanoparticles/reduced graphene oxide nanocomposites for catalytic reduction of 4-nitrophenol, organic dyes and act as energy storage electrode material

2019, Composites Part B: Engineering

Show abstract

View all citing articles on Scopus

View Abstract